A Study on the Propagation of Measurement Uncertainties into the Result on a Turbine Performance Test

Soo-Yong Cho*, Chanwoo Park
Department of Mechanical and Aerospace Engineering Gyeongsang National University, Jinju, Gajoa-dong 900, Gyeongnam 660-701, Korea

Uncertainties generated from the individual measured variables have an influence on the uncertainty of the experimental result through a data reduction equation. In this study, a performance test of a single stage axial type turbine is conducted, and total-to-total efficiencies are measured at the various off-design points in the low pressure and cold state. Based on an experimental apparatus, a data reduction equation for turbine efficiency is formulated and six measured variables are selected. Codes are written to calculate the efficiency, the uncertainty of the efficiency, and the sensitivity of the efficiency uncertainty by each of the measured quantities. The influence of each measured variable on the experimental result is figured out. Results show that the largest uncertainty magnification factor (UMF) value is obtained by the inlet total pressure among the six measured variables, and its value is always greater than one. The UMF values of the inlet total temperature, the torque, and the RPM are always one. The uncertainty percentage contribution (UPC) of the RPM shows the lowest influence on the uncertainty of the turbine efficiency, but the UPC of the torque has the largest influence to the result among the measured variables. These results are applied to find the correct direction for meeting an uncertainty requirement of the experimental result in the planning or development phase of experiment, and also to offer ideas for preparing a measurement system in the planning phase.

Key Words : Uncertainty, Axial Type Turbine, Uncertainty Magnification Factor, Uncertainty Percentage Contribution, Turbine Performance Test

Nomenclature

B : Bias error
b : Blade height
Ca : Absolute axial flow velocity
Cp : Specific heat at constant pressure
c_s : Chord length of stator
h : Enthalpy
Δh_t : Stagnation enthalpy drop in a stage
J : Conversion factor
$\dot{m}$: Mass flow rate
P : Pressure
R : Precision error
Tq : Torque
U : Uncertainty
V : Velocity at free stream
S : Pitch
x : Measured variable
y : Pitchwise direction

Greek Symbols

α : Absolute flow angle
γ : Specific heat ratio
Λ : Degree of reaction
η : Efficiency
λ : Blade speed
ν : Dynamic viscosity
ρ : Density
σ : P/P_{std}

* Corresponding Author,
E-mail : sycho@gsnu.ac.kr
TEL : +82-55-751-6106; **FAX** : +82-55-757-5622
Department of Mechanical and Aerospace Engineering Gyeongsang National University, Jinju, Gajoa-dong 900, Gyeongnam 660-701, Korea. (Manuscript **Received** July 31, 2003; **Revised** January 19, 2004)

θ : T/T_{std}
φ : Flow coefficient
Ψ : Blade loading coefficient
Ω : RPM

Subscripts

0 : Inlet of stator
1 : Exit of stator
2 : Exit of rotor
t : Total state
s : Static state

1. Introduction

In developing a new turbine system or core components to improve its performance, previous experimental results of components as well as those of the same class turbines have an important role. Moreover, experimental results are utilized in the validation and development of turbine performance prediction codes, design codes, CFD codes, and blade optimization conducted by Cho et al.(2002) etc. In order to use the experimental results in an effective way, detailed measurement uncertainties of the experimental results should be analyzed and included in the results. However, more importantly the uncertainty analysis should be conducted during the planning and development phase of a measurement to meet a requirement for the accuracy of the experimental results In the development of a turbine system or its core parts, generally many performance tests are conducted in a low pressure and cold state to find out the characteristics of design or aerodynamic parameters on its system before carrying out an experiment at a real driven condition. The reason for this is that it could avoid any unstable situations, which may occur from a variety of experiments as well as limited funds. For these reasons, it is important to figure out the relationship between the uncertainties of the measured variables and the experimental results obtained in the low pressure and cold state.

In single sample experiments, means for describing and analyzing the uncertainty interval in each result was suggested by Kline and McClintock (1953). It is referred to as the root sum squares (RSS) method. Moffat (1982) introduced the concept of replication level, such as zeroth, first, and Nth order, according to different sources of uncertainty in order to aid in identifying which of the candidate terms should be retained in an uncertainty analysis. Kline (1985) showed how to use the uncertainty analysis to reduce errors on the experiments. On a convective heat transfer problem, Moffat (1985) illustrated how to apply the uncertainty analysis in the planning phase of experiment. It was shown that a choice of test and a data reduction procedure could have an important impact on the accuracy of the results. Two uncertainty models of 99% or 95% confidence levels were suggested by Abernethy et al.(1985). In their methods, bias and precision errors of the parameters were kept separate until the last step of computing the uncertainty of the result.

If errors of measured variables are not independent of each other, the covariance would be nonzero. Coleman and Steele (1987) considered these covariance terms in the uncertainty analysis. Steele and Coleman (1987) showed that the accuracy of the experimental results depended on the method for making the measurements. ISO guide (1993) categorized into type A and B depending on the statistical analysis of series of observations instead of categorizing as bias or precision errors. Coleman and Steels (1995) used a coverage factor to obtain the expanded uncertainty in the ISO guide. The value of the coverage factor corresponds to the confidence level t value from the t-distribution and the effective number of degree of freedom for determining the t value is obtained from the Welch-Satterthwaite formula.

In evaluating the performance of a turbine, there are many methods as being used many equations for expressing the turbine efficiency. However, it depends on the characteristics of the experimental apparatus and the properties measured on a performance test. On the experiment in the low pressure and cold state, usually the total-to-total efficiency is adapted for evaluation with measuring the turbine output

power. In this study, the total-to-total efficiencies of a single stage axial type turbine at the off-design points are measured in the low pressure and cold state, and show how to relate with the uncertainties of the measured variables. These results could apply to find the correct direction for meeting an uncertainty requirement on the turbine performance test, and to offer ideas for preparing a measurement system in the planning and development phase of experiment.

2. Experimental Apparatus

The schematic diagram of the experimental apparatus applied in this study is illustrated in Fig. 1. The applied turbine is a single stage axial type turbine and it has 31 stator and 41 rotor blades. The solidity of the stator and rotor is 0.8 and 0.7, respectively. The stator has a 1.43 aspect ratio and the rotor has a 1.64 ratio. Detailed blade profiles are referred to Kim and Cho (2002). At the design point, this turbine is designed not to generate the swirl at exit. Table 1 shows the aerodynamic parameters at the design point.

The total pressure, static pressure and total temperature at the turbine inlet are measured at location 2 in Fig. 1, which is located at the distance of $2c_s$ upstream from the leading edge of the stator. At this location, the boundary layer thickness and the turbulent intensity are measured to find out the displacement thickness built up by the boundary layer. Table 2 shows the inlet flow state at 1.38×10^5 Reynolds number based on the blade height.

The total pressure and temperature at the turbine exit are measured at location 5 in Fig. 1, which is located at the distance of $7c_s$ downstream from the trailing edge of the rotor. The reason for setting up the long distance to measure at exit is that wakes generated from the rotor are completely disappeared at this distance. As a reference, Fig. 2 shows the decay of the wake generated on the trailing edge of the stator along downstream from the total pressure loss profiles. It shows the strength of wake is quickly decaying out as it goes far downstream, i.e., a 17% total

Table 1 Aerodynamics parameters at the design point

Stator exit flow angle (α_1)	37.3°
Flow coefficient ($\varphi=Ca/\lambda$)	1.68
$\Lambda=(h_1-h_2)/(h_0-h_2)$	0.373
$\Psi=2\Delta h_t/\lambda^2$	2.55
$\dot{m}\sqrt{\theta}/\sigma$	1.35
$\Omega/\sqrt{\theta}$	1784
Mean diameter	257.6 mm

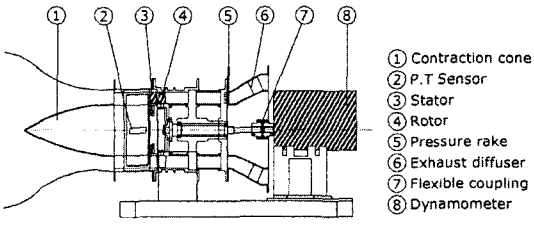

Fig. 1 Schematic diagram of experimental apparatus

Table 2 *Inlet flow conditions when axial velocity is* 45 m/sec

Boundary layer thickness (δ/b)	0.042
Displacement thickness (δ^*/b)	1.0×10^{-2}
Momentum thickness (ζ/b)	6.08×10^{-3}
Shape factor ($H=\delta^*/\zeta$)	1.64
Reynolds No. (Vb/ν)	1.38×10^5
Turbulent intensity at free stream	0.7%
Max. turbulent intensity (within boundary layer)	7.5%

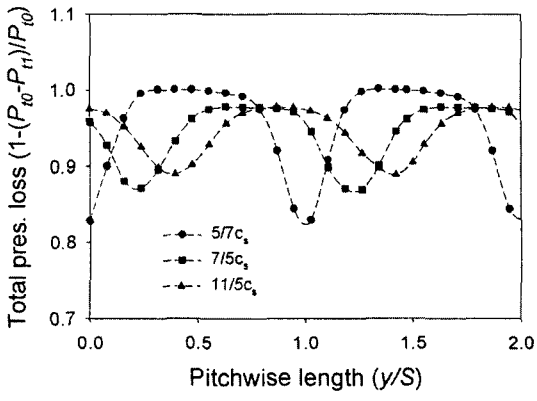

Fig. 2 Total pressure loss profiles along the axial direction from the trailing edge of the stator

pressure loss at $5/7C_s$ is decreased to 10% at $11/5C_s$. However, the flow angle at exit is not always zero because of the swirl generated on the operation at the off-design points. Fig. 3 shows the various flow angles at the location of $7C_s$ downstream from the trailing edge of the rotor. In order to measure the exit total pressure accurately, 4 rakes are used and each has 6 pressure taps. They are set up according to the exit flow angle.

The output power is measured by a dynamometer connected directly to the turbine shaft. The torque, RPM, temperature and pressure are saved in a data logger simultaneously. From these measured variables, the total-to-total efficiency is calculated using Eq. (1).

$$\eta_{t-t}=\frac{TqQ}{JCT_{t0}(\Delta P)^{1/2}\left[1-\left(\frac{P_{t2}}{P_{t0}}\right)^{\frac{\gamma-1}{\gamma}}\right]} \quad (1)$$

where C is $C_p\tilde{A}\rho^{1/2}$ and $\tilde{A}$ is a cross sectional area calculated by eliminating the displacement thickness at inlet. ΔP means the pressure difference between the total and static at inlet.

Evaluating the total-to-total efficiency of the turbine, six variables should be measured on the performance test, i.e., the torque (Tq), RPM (Q), inlet total temperature (T_{t0}), inlet total pressure (P_{t0}), inlet static pressure (P_{s0}) and exit total pressure (P_{t2}). Others except six variables assume constant because the experiment is conducted in the low pressure and cold state. The total-to-total efficiency includes some uncertainty because the measurement uncertainty of each variable is propagated through the data reduction equation (DRE). Therefore, it is important to control effectively the uncertainty of the measured variables for the accuracy of the experimental results in the planning phase.

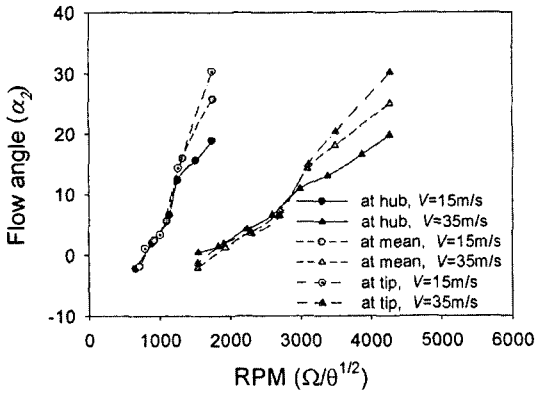

Fig. 3 Variation of absolute flow angle at the exit of the rotor due to the swirl generated at the off-design points

3. Results and Discussions

Each measured value includes the measurement error, which would combine in some manner with other errors to increase the uncertainty of the measurement. Consider a measurement of x which is subject to M elements of error e_j, where $j=1, \cdots, M$. A realistic estimate of uncertainty in the measurement due to these elemental errors can be computed using the RSS.

$$U_x=\pm\sqrt{\sum_{j=1}^{M}e_j^2} \quad (2)$$

The RSS method of combining errors is based on the assumption that the possible variations in the values of an error encountered over repeated measurements will tend to follow a Gaussian distribution. Measured variables are commonly used with a functional relationship to determine some resultant value. The most probable estimate of the resultant uncertainty is generally accepted as a value given by the second power law suggested by Kline and McClintock (1953). The second power laws can be derived from the linearized approximation of Taylor series expansion of the multivariable function. The propagation of uncertainty in the variables to the result will yield an uncertainty estimate as Eq. (3).

$$U_R^2=\sum_{i=0}^{N}(\xi_i U_{x_i})^2 \quad (3)$$

where a sensitivity index (ξ_i) relates how changes in each measured variable x_i affect the result.

The uncertainty of each measured variable can be calculated from the measurement errors which could be classified into the bias or systematic errors (B) and the precision or random errors (R). If there is no correlation between the bias

error and the random error, each error will be calculated by summing up linearly.

$$B_R^2=\sum_{i=1}^{N}\left[(\xi_i B_{x_i})^2+\sum_{k=1}^{N}\xi_i\xi_k B_{x_i}B_{x_k}(1-\delta_{ik})\right] \quad (4a)$$

$$R_R^2=\sum_{i=1}^{N}\left[(\xi_i R_{x_i})^2+\sum_{k=1}^{N}\xi_i\xi_k R_{x_i}R_{x_k}(1-\delta_{ik})\right] \quad (4b)$$

where δ_{ik} is the Kronecker delta function. The uncertainty of the result is calculated with the t-distribution on the precision error.

$$U_R^2=B_R^2+(t_v R_R)^2 \quad (5)$$

The t-distribution value for 95% confidence level is a function of the degree of freedom. For large samples, i.e., N>30, t is set equal to 2, otherwise the Welch-Satterthwaite formula is used. The measurement uncertainty of each variable is varied according to the off design points. Only for a reference about the uncertainties of measured variables, table 3 shows them in the condition of a 1.29 flow coefficient and 3.16 non-dimensional turbine input power. The non-dimensional input power is defined as follows;

$$\frac{\Delta h_t}{T_{t0}}=C_p\left[1-\left(\frac{P_{t2}}{P_{t0}}\right)^{\frac{\gamma-1}{\gamma}}\right] \quad (6)$$

Fig. 4 shows contours of the total-to-total efficiency. To obtain the contours, experiments are conducted at 195 different off design points. Each point has 35 samples for each measured variable and the result is validated through three full experiments. The low efficiency region is related with the part load, which has a low value at high RPM. In order to show the variation of the total-to-total efficiency more clearly at constant non-dimensional input powers, two dimensional curves are drawn in Fig. 5. They show the maximum efficiency is obtained at the RPM and input power on the design point.

For the calculation of uncertainty of the total-to-total efficiency, the DRE is used, and the RSS method is applied with the uncertainty of measured variables. Fig. 6 shows contours of the uncertainty of the total-to-total efficiency, which is obtained using Eq. (7). They have an upward trend with decreasing the input power. This comes from the low efficiency in the region of low input power. However, the uncertainties of the measured variables have almost the same magnitude in the overall experimental region. Therefore, the lowest uncertainty of the efficiency is shown in the region of design point.

$$\frac{U_{\eta_{t-t}}}{\eta_{t-t}}=\pm\left[\sum_{i=1}^{6}\left(\frac{x_i}{\eta_{t-t}}\frac{\partial\eta_{t-t}}{\partial x_i}\right)^2\left(\frac{U_{x_i}}{x_i}\right)^2\right]^{1/2} \quad (7)$$

Codes are written to calculate the efficiency,

Table 3 Uncertainties of measured variables in a 1.29 flow coefficient and 3.16 non-dimensional turbine input power state

	B_x	R_x	U_x
Ω(RPM)	±0.5 (resolution) ±6.79 (cal. curve)	3.90	10.36
Tq (kg_f.cm)	±0.525 (cal. curve) ±0.03%@R.O (combined) ±0.02%@R.O (non-repeatability) ±0.03%@R.O (creep)	0.084	0.56
P_{t0} (Pa)	±0.003%@F.S (resolution) ±0.15%@F.S (static error) ±0.0015%@F.S (thermal effect) ±0.001%@F.S (line pressure effect)	1.12	10.55
P_{s0} (Pa)	same to P_{t0}	0.76	10.42
P_{t2} (Pa)	same to P_{t0} ±0.5%@R.O (turning angle effect)	0.79	10.62
T_{t0} (K)	±2.25 (cal. curve) ±0.01 (accuracy)	0.11	2.26

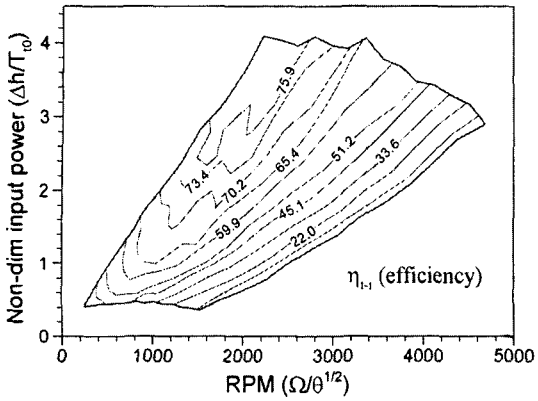

Fig. 4 Contours of total-to-total efficiency with various non-domensional input power and RPM

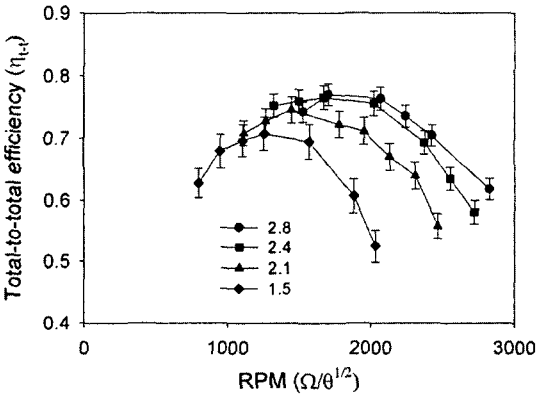

Fig. 5 Total-to-total efficiency curves with uncertainty bands at constant non-dimensional input powers

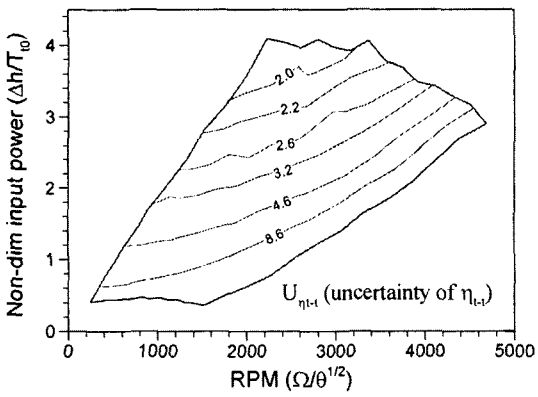

Fig. 6 Uncertainties of total-to total efficiency at the off-design points

the uncertainty of the efficiency, and the sensitivity of the efficiency uncertainty from each of the measured quantities. There are two ways to express the sensitivity of the result uncertainty by the uncertainty of the various measured quantities, i.e., uncertainty magnification factor (UMF) and uncertainty percentage contribution (UPC). The UMF of the measured variables x_i is defined in Eq. (8).

$$UMF\_x_i=\frac{x_i}{\eta_{t-t}}\frac{\partial\eta_{t-t}}{\partial x_i} \tag{8}$$

The UMF illustrates the influence of the uncertainty on one variable as it propagates through the DRE into the result if the uncertainties of all other variables are ignored. The significance of the UMF can be seen by referring to Eq. (7). If the UMF is less than one, the variable uncertainty diminishes as it propagates through the DRE; if the UMF is greater than 1, the variable uncertainty increases as it propagates through the DRE. All UMF values are presented as positive numbers because the sign does not affect the overall uncertainty since all terms are squared in the uncertainty equation. This type of analysis is useful for a general case during the planning phase of an experiment. The UMF of the inlet total pressure is obtained in Eq. (9).

$$UMF\_P_{t0}=\frac{P_{t0}}{2(P_{t0}-P_{s0})}+\frac{\frac{\gamma-1}{\gamma}}{\left[\left(\frac{P_{t0}}{P_{t2}}\right)^{\frac{\gamma-1}{\gamma}}-1\right]} \tag{9}$$

From Eq. (9), one knows that the UMF of the inlet total pressure has a close relationship with the expansion ratio, and also it is expected that its value would be large on the experiment in the low pressure and cold state. Fig. 7 shows the comparison of the UMF of the inlet total pressure, the exit total pressure, and the inlet static pressure. Among them, the UMF of the inlet total pressure has the largest value. Additionally, it always represents a greater value than those of other pressure variables. It is consistent with the UMF of the pressure variables, which is increased with decreasing the input power. This is directly related with the expansion ratio on the turbine. The other UMF values of the inlet total tempera-

ture, the torque, and the RPM are always 1. From these, one knows that the uncertainty of pressure variables should be controlled properly during the experiment with the low expansion ratio.

The UPC illustrates the influence of each variable and its uncertainty as a percentage contribution of the squared uncertainty in that variable to the squared uncertainty in the result. The UPC is defined as Eq. (10). The significance of the UPC can be seen by referring to Eq. (7). This analysis shows the sensitivity of the result uncertainty by the uncertainty of each variable for a particular situation. Since the UPC of a variable includes the effects of both the UMF and the uncertainty magnitude of the variable, it is useful in the planning phase once the uncertainties for each variable have been estimated. This usually follows an initial analysis of the UMF.

$$UPC\_x_i = \frac{\left(\frac{\partial \eta_{t-t}}{\partial x_i} U_{x_i}\right)^2}{\sum_{j=1}^{6}\left(\frac{\partial \eta_{t-t}}{\partial x_j} U_{x_j}\right)^2} \times 100 \qquad (10)$$

Figures 8 and 9 show contours of the UPC of the total pressure variables at inlet and exit, respectively. They show the influence of the uncertainty by the inlet total pressure on the result is greater than that of the exit total pressure. Fig. 8 shows the UPC of the inlet total pressure decreases with increasing the RPM at the constant input power; however, it increases with increasing the input power at the constant RPM. Even though the effect of the exit total pressure is similar to that of the inlet total pressure, the UPC of the exit total pressure is less than 8% in the whole measurement region. The reason for these is that the UPC depends on the UMF in the same measurement and operating condition.

The UPC of the inlet total temperature is shown in Fig. 10, and the contours of the UPC of the inlet static pressure are shown in Fig. 11. The UPC of the inlet total temperature decreases with increasing the RPM at the constant input power; however, it increases with increasing the input power at the constant RPM. One knows that the UPC of the inlet static pressure shows the similar trend like that of the inlet total temperature. However, the most influenced UPC

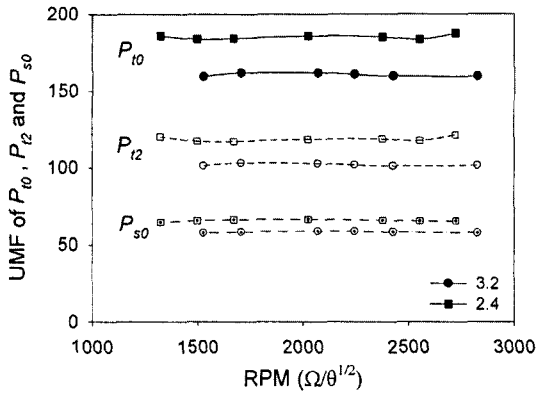

Fig. 7 Comparison of uncertainty magnification factors by inlet total pressure, inlet static pressure, and exit total pressure parameters

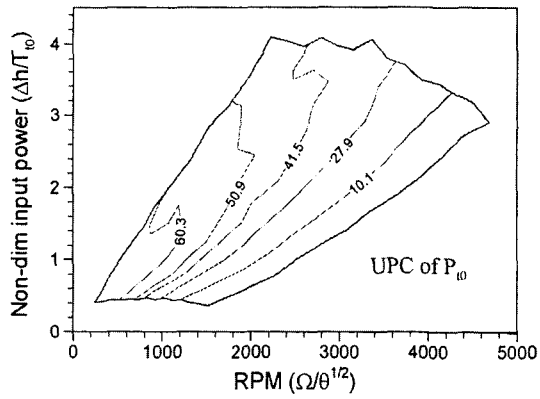

Fig. 8 Uncertainty percentage contribution of inlet total pressure parameter

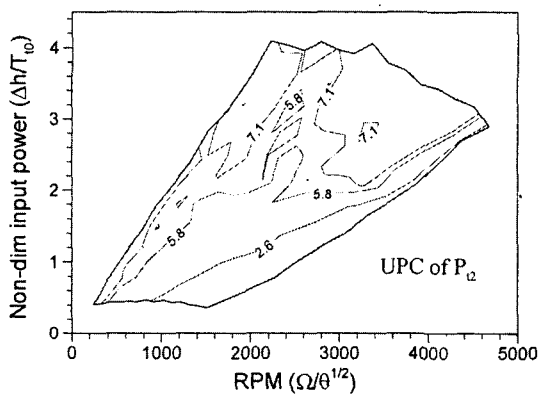

Fig. 9 Uncertainty percentage contribution of exit total pressure parameter

region is different, i. e., in case of the inlet total temperature, it varies with the input power proportionally but the RPM reversely. For the inlet static pressure, it appears in the region where the RPM and the input power are decreased. From comparison between the two results, it shows that the influence to the result is a little larger by the inlet total temperature than the inlet static pressure. It is caused by applying the bias error to 0.75% of the reading assumed generally on the temperature measurement as recommended by ANSI. Hudson and Coleman (1996) showed the low effect of the inlet total temperature to the result without considering above bias error on the temperature measurement, i.e., its effect was less than 2% for the whole region. From these, one recognizes that some different result could be caused by the data reduction procedure.

Figure 12 shows the UPC of the torque. It has a strong influence on the high RPM, but its effect is quickly reduced with decreasing the RPM. The reason is that the measured torque increases with decreasing the RPM, so its relative value decreases with the given uncertainty of the torque. As a similar phenomenon, the UPC of the torque increases with decreasing the input power. From these results, one recognizes that the UPC value is directly related to the value of the measured variable from the relationship between the UPC and the UMF equation even though the UMF value is 1. Fig. 13 shows the UPC of the RPM and it shows the same trend

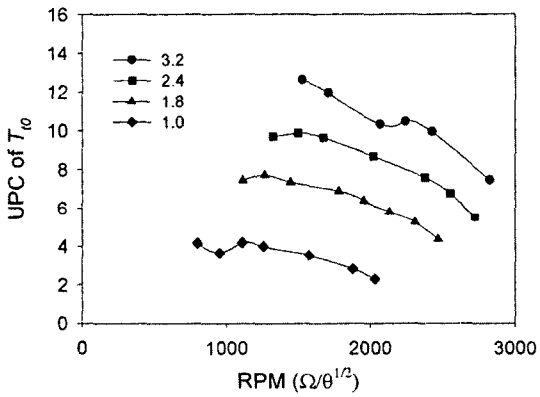

Fig. 10 Uncertainty percentage contribution of inlet total temperature parameter with constant non-dimensional input powers

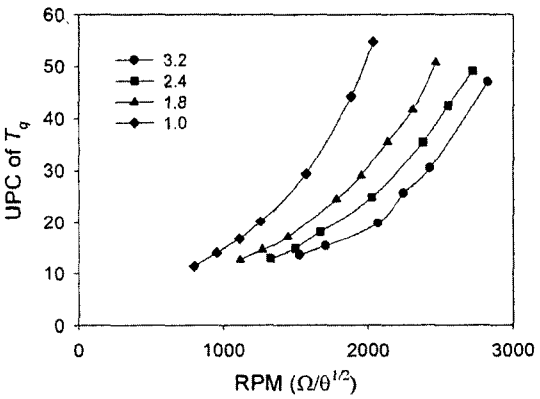

Fig. 12 Uncertainty percentage contribution of torque parameter with constant non-dimensional input powers

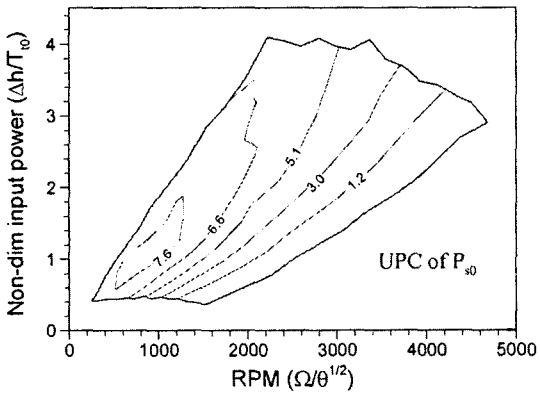

Fig. 11 Uncertainty percentage contribution of inlet static pressure parameter

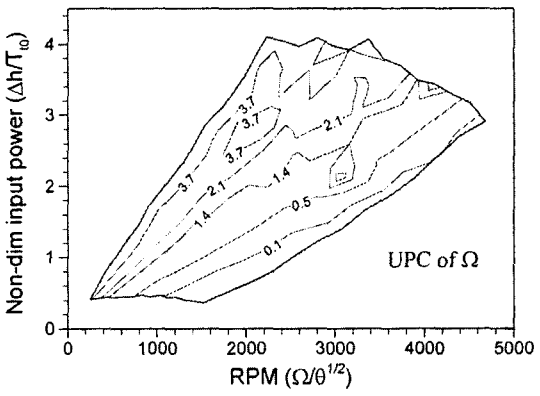

Fig. 13 Uncertainty percentage contribution of RPM (Ω) parameter

like the UPC of the torque. It has the lowest effect to the result, and its values are less than 5% for the whole experimental region.

4. Conclusions

(1) In the experiment of a single stage axial type turbine in the low pressure and cold state, the influences of the measured variables on the uncertainty of the total-to-total efficiency are figured out. The UMF values of the pressure variables are always greater than one, and especially the UMF of the inlet total pressure shows the largest value. However, these can be alleviated on the experiment in the medium or high pressure state because the UMF values of the pressure variables are related with the expansion ratio. Other UMF values of measured variables, such as the torque, RPM and inlet total temperature, are always one. This means that the pressure measurements are critical for obtaining the turbine efficiency accurately.

(2) The UPC of the pressure variables shows that it decreases with increasing the RPM at constant input power ; however, it increases with increasing the input power at constant RPM. The influence of the uncertainty by the inlet total pressure is greater than those of other pressure variables. The UPC values of the exit total pressure and inlet static pressure are less than 8% for the whole measurement region. In the same measurement and operating condition, the UPC depends on the UMF.

(3) The UPC of the RPM shows the lowest influence on the uncertainty of turbine efficiency, but the UPC of the torque has the largest influence on the result among the measured variables. These results show that the UPC of the torque is quickly reduced with increasing the torque, and also the UPC of the RPM decreases with increasing the RPM. It means that the UPC value is directly related with the value of the measured variables.

(4) Experimental results are useful for finding the correct direction to meet the uncertainty requirement of the experimental result in the planning or development phase of experiment, and selecting any measured variables to be controlled. As future work, an analysis with other DRE formulas expressing the turbine efficiency would be considered.

Acknowledgment

Authors would like to acknowledge the financial support from the ReCAPT (Research Center for Aircraft Parts technology) and the Brain Korea 21 Project.

References

Abernethy, R. B., Benedict, R. P. and Dowdell, R. B., 1985, "ASME Measurement Uncertainty," *J. of Fluids Engineering*, Vol. 107, pp. 161～164.

Cho, S. Y., Yoon, E. S. and Choi, B. S., 2002, "A Study on an Axial-Type 2-D Turbine Blade Shape for Reducing the Blade Profile Loss," *KSME Int. J.*, Vol. 16, No. 8, pp. 1154～1164.

Coleman, H. W. and Steels, W. G., 1987, "Some Considerations in the Propagation of Bias and Precision Errors into an Experimental Results," FED-Vol. 58, pp. 57～62.

Coleman, H. W. and Steels, W. G., 1995, "Engineering Application of Uncertainty Analysis," *AIAA, J.*, Vol. 33, No. 10, pp. 1888～1896.

Hudson, S. T and Coleman, H. W., 1996, "A Preliminary Assessment of Methods for Determining Turbine Efficiency," AIAA 96-0101, Reno.

International Organization for Standardization, 1993, "Guide to the Expression of Uncertainty in Measurement," ISBN 92-67-10188-9, ISO, Geneva.

Kim, D. S. and Cho, S. Y., 2002, "An Experimental Study of Incidence Angle Effect on 3-D Axial Type Turbine," *Trans of KSME (B)*, Vol. 26, No. 9, pp. 1291～1301.

Kline, S. J. and McClintock, F. A. 1953, "Describing Uncertainties in Single-Sample Experiments," *Mech. Eng.*, Jan., pp. 3～8.

Kline, S. J., 1985, "The Purposes of Uncertainty Analysis," *J. of Fluids Engineering*, Vol. 107, pp. 153～160.

Moffat, R. J., 1982, "Contributions to the The-

ory of Single-Sample Uncertainty Analysis," *J. of Fluids Engineering*, Vol. 104, pp. 250~260.

Moffat, R. J., 1985, "Using Uncertainty Analysis in the Planning of an Experiment," *J. of Fluids Engineering*, Vol. 107, pp. 173~178.

Moffat, R. J., 1988, "Describing the Uncertainties in Experimental Results," *Experimental Thermal and Fluid Science*, Vol. 1, pp. 3~17.

Steels, W. G. and Coleman, W. G., 1987, "Use of Uncertainty Analysis in the Planning and Design of an Experiment," FED-Vol. 58, pp. 63~67.